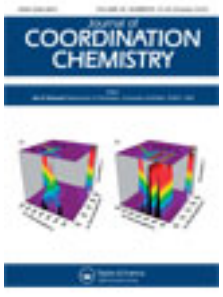

Journal of Coordination Chemistry
Publication details, including instructions for authors and subscription information:
http://www.tandfonline.com/loi/gcoo20

Syntheses, crystal structures, and magnetic properties of the banana-shaped tungstophosphates: $[M_6(H_2O)_2(PW_9O_{34})_2(PW_6O_{26})]^{17-}$ (M^{II}=Ni^{II}, Co^{II})

Lei Yang [a b], Juan Zhao [a], Junwei Zhao [a] & Jingyang Niu [a]
[a] Institute of Molecular and Crystal Engineering, College of Chemistry and Chemical Engineering, Henan University, Kaifeng, Henan 475004, P.R. China
[b] The Department of Physics-Chemistry, Henan Polytechnic University, Jiaozuo, Henan 454150, P.R. China
Accepted author version posted online: 24 Jul 2012.Published online: 13 Sep 2012.

To cite this article: Lei Yang, Juan Zhao, Junwei Zhao & Jingyang Niu (2012) Syntheses, crystal structures, and magnetic properties of the banana-shaped tungstophosphates: $[M_6(H_2O)_2(PW_9O_{34})_2(PW_6O_{26})]^{17-}$ (M^{II}=Ni^{II}, Co^{II}), Journal of Coordination Chemistry, 65:19, 3363-3371, DOI: 10.1080/00958972.2012.715344

To link to this article: http://dx.doi.org/10.1080/00958972.2012.715344

Journal of Coordination Chemistry
Vol. 65, No. 19, 10 October 2012, 3363–3371

Syntheses, crystal structures, and magnetic properties of the banana-shaped tungstophosphates: $[M_6(H_2O)_2(PW_9O_{34})_2(PW_6O_{26})]^{17-}$ (M^{II} = Ni^{II}, Co^{II})

LEI YANG†‡, JUAN ZHAO†, JUNWEI ZHAO† and JINGYANG NIU*†

†Institute of Molecular and Crystal Engineering, College of Chemistry and Chemical Engineering, Henan University, Kaifeng, Henan 475004, P.R. China
‡The Department of Physics-Chemistry, Henan Polytechnic University, Jiaozuo, Henan 454150, P.R. China

(*Received 21 February 2012; in final form 26 June 2012*)

Two new banana-shaped tungstophosphates $[M_6(H_2O)_2(PW_9O_{34})_2(PW_6O_{26})]^{17-}$ (M^{II} = Ni^{II}, Co^{II}) incorporating two types of lacunary polyoxometalate units have been synthesized in aqueous solution and characterized by elemental analyses, IR, and UV spectra, and single-crystal X-ray diffraction. Structural analyses show that $Na_6H_{11}[Ni_6(H_2O)_2(PW_9O_{34})_2(PW_6O_{26})]\cdot 32H_2O$ (**1**) and $Na_7H_{10}[Co_6(H_2O)_2(PW_9O_{34})_2(PW_6O_{26})]\cdot 31H_2O$ (**2**) are generated from two tri-M^{II} substituted B-α-$[(MOH_2)M_2PW_9O_{34}]$ Keggin units connected by a hexavacant $[PW_6O_{26}]^{11-}$ Keggin fragment, leading to the M^{II}-containing banana-shaped tungstophosphates. Magnetic properties of **2** show decrease of the molar magnetic susceptibility at higher temperatures results from spin-orbit coupling of Co^{II} and antiferromagnetic interactions whereas the maximum at the lower temperatures is indicative of the ferromagnetic interactions within the trinuclear Co^{II} spin cluster in the sandwich belt.

Keywords: Banana-shaped; Magnetism; Tungstophosphates

1. Introduction

Polyoxometalates (POMs), with versatile structural topologies, nucleophilic oxygen-enriched surfaces, and redox, photo and magnetic properties, represent excellent candidates for the development of nanomolecules based on the building-block strategy [1–3]. Keggin, Dawson, and Anderson moieties have been widely used as building blocks to construct extended structures by different linkers such as d- and f-block cations [4–8]. Attention has concentrated on highly charged lacunary species, which are able to act as bulky multidentate ligands for incorporation of multiple transition-metal ions, leading to a family of transition metal-substituted polyoxotungstates (TMSPs) with various stoichiometries and structural features combined with interesting catalytic and magnetic properties [9, 10]. Compared with abundant reports of dimeric sandwich-type complexes $[M_x(XW_9)_2]^{n-}$ or $[M_x(X_2W_{15})_2]^{m-}$ ($x = 2$–6) [11–17], POM architectures consisting of two different polyainon subunits are rare, only several asymmetric

*Corresponding author. Email: jyniu@henu.edu.cn

ISSN 0095-8972 print/ISSN 1029-0389 online © 2012 Taylor & Francis
http://dx.doi.org/10.1080/00958972.2012.715344

sandwich-type POMs encapsulating two nonequivalent Keggin fragments were observed: *S*-shaped POMs $[\{(B\text{-}\beta\text{-}SiW_9O_{33}(OH))(\beta\text{-}SiW_8O_{29}(OH)_2)Co_3(H_2O)\}_2Co(H_2O)_2]^{20-}$ [18], $[Mn(H_2O)_2\{Mn_3(H_2O)(B\text{-}\beta\text{-}GeW_9O_{33}(OH)(B\text{-}\beta\text{-}GeW_8O_{30})(OH)\}_2]^{22-}$ [19], $[K(H_2O)(\beta Fe_2GeW_{10}O_{37}(OH))(\gamma\text{-}GeW_{10}O_{36})]^{12-}$ [20], $[enH_2]_2[(\alpha\text{-}H_2As^VW_6O_{26})Fe_3(H_2O)(B\alpha\text{-}H_4As^VW_9O_{34})]_2[Fe]_2\cdot 8H_2O$ [21], and $[Ni_7(OH)_4(H_2O)(CO_3)_2(HCO_3)(A\text{-}\alpha\text{-}SiW_9O_{34})(\beta SiW_{10}O_{37})]^{10-}$ [22]. Since the first banana-shaped TMSP $[Co_7(H_2O)_2(OH)_2P_2W_{25}O_{94}]^{16-}$ was discovered by Coronado *et al.* [23], several banana-shaped tungstophosphates were reported, for instance, $[Ni_4Mn_2P_3W_{24}O_{94}(H_2O)_2]^{17-}$ [24], $[Mn_6P_3W_{24}O_{94}(H_2O)_2]^{17-}$ [25], $[M_6(H_2O)_2(AsW_9O_{34})_2(AsW_6O_{26})]^{17-}$ ($M^{II}=Ni^{II}$, Mn^{II}, Co^{II}, Zn^{II}) [26], $[(Fe_4W_9O_{34}(H_2O)_2(FeW_6O_{26})]^{19-}$ [27], and $[M_6Ge_3W_{24}O_{94}(H_2O)_2]^{n-}$ ($M=Fe^{III}$, $n=14$; $M=Co^{II}$, $n=20$; $M=Mn^{II}/Mn^{III}$, $n=18$) [28–30].

To seek the most promising strategies for constructing TMSPs with novel structures and good properties, we launched explorations on high nuclear TMSPs by selecting appropriate POMs precursors and TM ions. In previous works, we reported two organic–inorganic hybrid Ni^{II}-substituted tungstoarsenates $\{[Ni_3(dap)(H_2O)_2]_2(H_2W_4O_{16})\}\{(\alpha H_2AsW_6O_{26})[Ni_6(OH)_2(H_2O)(dap)_2](B\text{-}\alpha\text{-}HAsW_9O_{34})\}_2]^{8-}$ [31] and $(H_2en)_4H_{20}\{Co(Hen)[Co_6As_3W_{24}O_{94}(H_2O)_2]\}_2\cdot 15H_2O$ (en = ethylenediamine) [32], which represents the first example of 1-D chain inorganic–organic hybrids containing double banana-shaped polyoxoanions. As continuation of our work, herein, we report another two new banana-shaped TMSPs, $Na_6H_{11}[Ni_6(H_2O)_2(PW_9O_{34})_2(PW_6O_{26})]\cdot 32H_2O$ (**1**) and $Na_7H_{10}[Co_6(H_2O)_2(PW_9O_{34})_2(PW_6O_{26})]\cdot 31H_2O$ (**2**).

2. Experimental

2.1. *Materials and methods*

All chemicals are analytical grade and used without purification. Inductively coupled plasma (ICP) spectra were performed on a Perkin-Elmer Optima 2000 ICP-OES spectrometer. IR spectra were obtained from KBr pellets on a Nicolet 170 SXFT-IR spectrometer from 400 to 4000 cm^{-1}. UV absorption spectra were obtained with a U-4100 spectrometer at room temperature. Thermogravimetric analyses were performed in N_2 on a Perkin-Elmer-7 instrument with a heating rate of $10^{\circ}C\,min^{-1}$. XRPD measurements were performed on a Philips X'Pert-MPD instrument with CuKα radiation ($\lambda=1.54056$ Å) at 293 K. Magnetic susceptibility measurements were obtained with a Quantum Design MPMS-XL7 SQUID magnetometer from 1.8 to 300 K.

2.2. *Synthesis of 1 and 2*

2.2.1. $Na_6H_{11}[Ni_6(H_2O)_2(PW_9O_{34})_2(PW_6O_{26})]\cdot 32H_2O$ (1). To a solution containing $Na_2WO_4\cdot 2H_2O$ (5.000 g, 15.16 mmol) in 10 mL distilled water, 85% H_3PO_4 (0.17 mL, 2.49 mmol) and CH_3COOH (0.5 mL, 8.75 mmol) were added with vigorous stirring, then a solution containing $Ni(CH_3COO)_2\cdot 4H_2O$ (0.248 g, in 3 mL distilled water) was added. The pH of the resulting solution was adjusted to 5.5 with CH_3COOH and refluxed for 20 min, then cooled to room temperature and filtered. After 9 days, green

crystals were collected (Yield: *ca* 74% based on $Ni(CH_3COO)_2 \cdot 4H_2O$). Elemental Anal. Calcd for $H_{79}Na_6Ni_6O_{128}P_3W_{24}$ (%): Na, 1.94; Ni, 4.94; P, 1.30; W, 61.94. Found (%): Na, 1.90; Ni, 5.01; P, 1.33; W, 61.87. [MW = 7123.14 g mol^{-1}]. IR (KBr pellet 4000–400 cm^{-1}): 525, 692, 731, 802, 895, 928, 1010, 1060, 1100, 1640, and 3450.

2.2.2. $Na_7H_{10}[Co_6(H_2O)_2(PW_9O_{34})_2(PW_6O_{26})] \cdot 31H_2O$ (2). Compound **2** was prepared using a method similar to that employed for synthesis of **1**, with $Co(CH_3COO)_2 \cdot 4H_2O$ in place of $Ni(CH_3COO)_2 \cdot 4H_2O$. After 8 days, purple block crystals were collected (Yield: *ca* 78% based on $Co(CH_3COO)_2 \cdot 4H_2O$). Nadjo and Hill have reported the structurally analogous Ni-containing complex $[Ni_4Mn_2P_3W_{24}O_{94}(H_2O)_2]$ [24] and Co-containing $[Co_6P_3W_{24}O_{94}(H_2O)_2]^{17-}$ [25]. However, these complexes were isolated through decomposition of the sandwich complex $[(M(OH_2)_2)_3(A\text{-}R\text{-}XW_9O_{34})_2]^{12-}$ precursor while **1** and **2** were obtained in higher yield by the reaction of $Na_2WO_4 \cdot 2H_2O$, H_3PO_4, CH_3COOH, and $M(CH_3COO)_2 \cdot 4H_2O$ ($M^{II} = Ni^{II}$, Co^{II}). Elemental Anal. Calcd for $H_{76}Na_7Co_6O_{127}P_3W_{24}$ (%): Na, 2.26; Co, 4.96; P, 1.30; W, 61.89. Found (%): Na, 2.31; Co, 4.87; P, 1.27; W, 61.83. [MW = 7128.43 g mol^{-1}]. IR (KBr pellet 4000–400 cm^{-1}): 488, 733, 798, 899, 931, 1030, 1640, and 3450.

2.3. *Crystallographic data collection and structure determination*

Structural analyses were performed on a Bruker APEX-II CCD diffractometer using graphite monochromated Mo-Kα radiation ($\lambda = 0.71073$ Å). The data were collected at 296 K. Data processing was accomplished with SAINT [33]. **1** and **2** were solved in the space group $P2_1/c$ by direct methods and refined on F^2 by full-matrix least-squares using SHELXTL 97 [34]. The heaviest atoms could be unambiguously located. Oxygen atoms were subsequently located in the difference Fourier maps. No hydrogen atoms associated with water were located in the difference Fourier map. All non-hydrogen atoms were refined with anisotropic thermal parameters. The final least-square cycle of refinement gave $R = 0.0278$, $wR = 0.0667$ for **1** and $R = 0.0590$, $wR = 0.1627$ for **2**. The crystallographic data, selected bond lengths and angles are listed in tables 1, S1, and S2, respectively.

3. Results and discussion

3.1. *IR spectra*

IR spectra of **1** and **2** are similar (figures S1 and S2), indicating the structural type of the polyoxoanions in **1** and **2** is almost the same, in good agreement with the results of X-ray diffraction structural analyses. The IR spectra show characteristic vibrations resulting from lacunary Keggin POM framework in the range 1100–700 cm^{-1}. Four characteristic bands attributed to ν(P–O), ν(W=Ot), ν(W–Ob), and ν(W–Oc) appear at 1095–1010, 928, 895–802, and 731 cm^{-1} for **1**; 1030, 933, 899–802, and 733 cm^{-1} for **2**, which are in agreement with reported tungstophosphate framework containing trivacant $[B\text{-}\alpha\text{-}PW_9O_{34}]^{9-}$ and hexavacant $[B\text{-}PW_6O_{26}]^{11-}$ fragments [25].

Table 1. Crystal data and structure refinement parameters for **1** and **2**.

Empirical formula	$H_{79}Na_6Ni_6O_{128}P_3W_{24}$ (**1**)	$H_{76}Co_6Na_7O_{127}P_3W_{24}$ (**2**)
Formula weight	7123.14	7128.43
Temperature (K)	296(2)	296(2)
Wavelength (Å)	0.71073	0.71073
Crystal system	Monoclinic	Monoclinic
Space group	$P2_1/c$	$P2_1/c$
Unit cell dimensions (Å, °)		
a	17.493(3)	17.617(6)
b	22.344(4)	22.411(7)
c	34.736(6)	34.900(11)
β	95.982(3)	96.011(5)
Volume (Å^3), Z	13,503(4), 4	13,703(8), 4
Calculated density (g cm^{-3})	3.504	3.455
Absorption coefficient (mm^{-1})	21.327	20.920
$F(000)$	12632	12608
Crystal size (mm^3)	$0.29 \times 0.25 \times 0.20$	$0.35 \times 0.27 \times 0.21$
θ range for data collection (°)	1.8–25	1.63–25
Limiting indices	$-17 \le h \le 20$; $-26 \le k \le 26$; $-41 \le l \le 40$	$-20 \le h \le 18$; $-26 \le k \le 25$; $-41 \le l \le 41$
Reflections collected	67,381	68,527
Independent reflection	23,709 [R(int) = 0.1215]	24,069 [R(int) = 0.1072]
Data/restraints/parameters	23,709/894/1508	24,069/882/1513
Goodness-of-fit on F^2	0.992	1.011
Final R indices [$I > 2\sigma(I)$]	$R_1 = 0.0795$, $wR_2 = 0.2000$	$R_1 = 0.0713$, $wR_2 = 0.1805$
R indices (all data)	$R_1 = 0.1405$, $wR_2 = 0.2269$	$R_1 = 0.1136$, $wR_2 = 0.2009$

$R_1 = \sum F_o| - |F_c| / \sum |F_o|$; $wR_2 = \{\sum[w(F_o^2 - F_c^2)^2] / \sum[w(F_o^2)^2]\}^{1/2}$.

In comparison with the IR spectrum of saturated Keggin tungstophosphate $Na_3PW_{12}O_{40} \cdot xH_2O$ [35], the ν(W = Ot) frequency has a red shift from the sandwiched M^{II} cations having stronger coordination interactions to the lacunary oxygen atoms of $[B\text{-}PW_9O_{34}]^{9-}$ and $[B\text{-}PW_6O_{26}]^{11-}$. The ν(W–Ob) and ν(W–Oc) frequencies also have red shifts from the decrease in symmetry of the banana-shaped $[M_6(H_2O)_2(PW_9O_{34})_2(PW_6O_{26})]^{17-}$ polyoxoanion compared with that of $Na_3PW_{12}O_{40} \cdot xH_2O$. The spectrum of **1** exhibits similar terminal W–O stretching and W–O–W bridging frequencies with **2**, but displays subtle differences in the intensities of these bands. Differences in the splitting of the vibration of the PO_4 units are seen for **1** relative to **2**. Most likely a combination of two factors is responsible. First, **1** and **2** contain two different types of phosphate groups by symmetry. Second, Jahn-Teller effects present for high spin Co^{II}, but not for Ni^{II}, may be responsible for changes in the splitting of PO_4 bands. Similar observations have been made for analogous Keggin sandwich species $[((MnOH_2)Mn_2PW_9O_{34})_2(PW_6O_{26})]^{17-}$ and $[((CoOH_2)Co_2PW_9O_{34})_2(PW_6O_{26})]^{17-}$ [25]. Vibrational bands at 3450 and 1640 cm^{-1} assigned to ν(O–H) and δ(O–H) of water molecules suggests the presence of the lattice water in **1** and **2**.

3.2. *Structural description*

X-ray powder diffraction patterns of **1** and **2** are consistent with those from the single-crystal structure analyses (figure S3), indicating phase purity. On the account of variation in preferred orientation of the powder sample in the experimental XRPD, intensities of the experimental and simulated XRPD patterns have some differences.

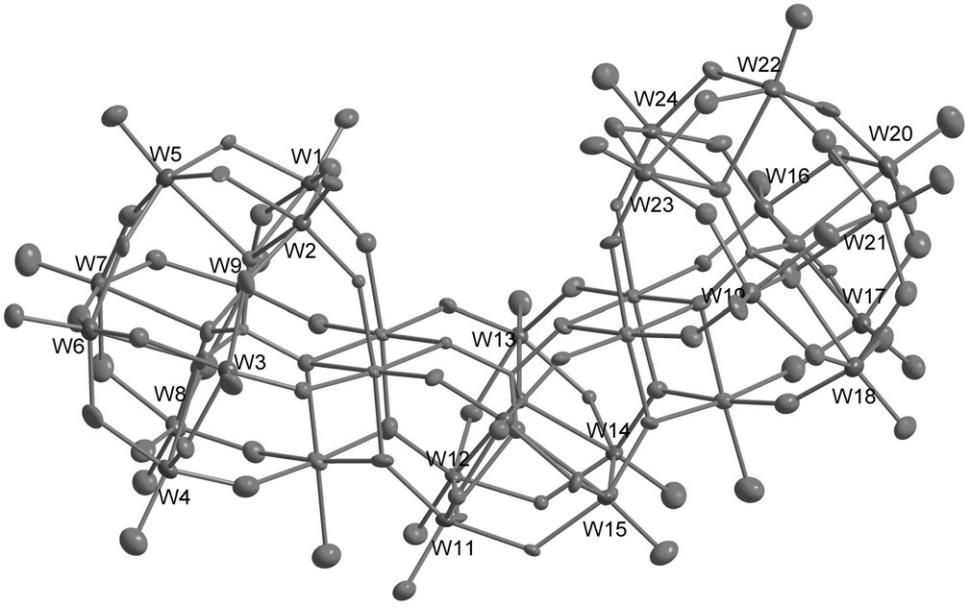

Figure 1. ORTEP plot of the asymmetric unit of **1** showing 50% probability thermal ellipsoids and the atom labeling scheme. Protons, sodium ions, and water molecules are omitted for clarity.

Single-crystal X-ray diffraction reveals that $[M_6(H_2O)_2(PW_9O_{34})_2(PW_6O_{26})]^{17-}$ (M^{II}=Ni^{II} for **1**; M^{II}=Co^{II} for **2**) display the same structural framework. Therefore, only the structure of **1** is described in detail.

The asymmetric unit of **1** (figure 1) consists of a banana-shaped polyoxoanion $[Ni_6P_3W_{24}O_{94}(H_2O)_2]^{17-}$, 11 protons, six sodium ions, and 32 lattice water molecules. The polyoxoanion $[Ni_6P_3W_{24}O_{94}(H_2O)_2]^{17-}$ (figure 2a) presents a banana-shaped structure with idealized C_{2v} symmetry composed of three kinds of units: trivacant $[B\text{-}PW_9O_{34}]^{9-}$ (figure 2b), $\{Ni_3O_{13}\}$ (figure 2c) and hexavacant $[B\text{-}PW_6O_{26}]^{11-}$ (figure 2d). $[B\text{-}PW_9O_{34}]^{9-}$ is formed by moving adjacent edge-sharing W_3O_{13} triads from a plenary α-Keggin $[PW_{12}O_{40}]^{3-}$ anion while $[B\text{-}PW_6O_{26}]^{11-}$ fragment is formed by moving two W_3O_{13} triads. The $\{Ni_3O_{13}\}$ unit is constituted by three edge-sharing NiO_6 octahedra. The B-α-$[(NiOH_2)Ni_2PW_9O_{34}]$ subunit is formed by a $[B\text{-}PW_9O_{34}]^{9-}$ and a $\{Ni_3O_{13}\}$ in corner-sharing motif and two such subunits are connected into the banana-shaped structure by $[B\text{-}PW_6O_{26}]^{11-}$ sharing the corner O with $\{Ni_3O_{13}\}$. The polyoxoanion can be considered as a double-sandwich structure, in which two $[B\text{-}PW_9O_{34}]^{9-}$ units and a $[B\text{-}PW_6O_{26}]^{11-}$ fragment are separated by two distinct $\{Ni_3O_{13}\}$ triads.

There are six crystallographically independent Ni^{II} centers from two $\{Ni_3O_{13}\}$ clusters. The six Ni^{II} all reside in octahedral geometries, displaying two kinds of octahedral environments: Ni3 and Ni6 have three oxygen atoms from $[B\text{-}\alpha\text{-}PW_9O_{34}]^{9-}$, two oxygen atoms from $[B\text{-}PW_6O_{26}]^{11-}$ and one terminal water [Ni–O: 1.99(2)–2.19(19) Å and Ni–OW: 2.02(2)–2.10(2) Å]; Ni1, Ni2, Ni4, and Ni5 are all bonded to six oxygen donors from $[B\text{-}\alpha\text{-}PW_9O_{34}]^{9-}$ and $[B\text{-}PW_6O_{26}]^{11-}$ [Ni–O: 1.956(17)–2.226(17) Å].

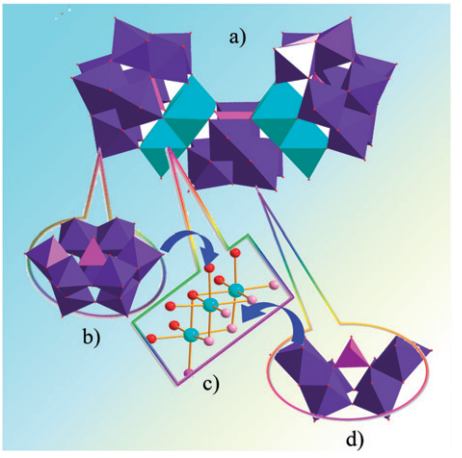

Figure 2. (Color online) (a) The polyhedral representation of banana-shaped M^{II}-substituted tungstophosphate anions: $[M_6(H_2O)_2(PW_9O_{34})_2(PW_6O_{26})]^{17-}$ (M^{II}=Ni^{II}, Co^{II}). Protons, sodium ions, and water molecules are omitted for clarity (Color code: WO_6, purple; PO_4, pink; NiO_6, sky blue; O, red). (b) B-$PW_9O_{34}]^{9-}$ formed by moving one adjacent edge-sharing W_3O_{13} from a plenary α-Keggin $[PW_{12}O_{40}]^{3-}$. (c) The $\{Ni_3O_{13}\}$ unit constituted by three edge-sharing NiO_6 octahedra (Color code: oxygen atoms sharing with the $[B\text{-}PW_9O_{34}]^{9-}$ unit, red; oxygen atoms sharing with the $[B\text{-}PW_6O_{26}]^{11-}$ unit, light pink; oxygen atoms from water, pink). (d) The $[B\text{-}PW_6O_{26}]^{11-}$ unit formed by moving two adjacent edge-sharing W_3O_{13} triads from a plenary α-Keggin $[PW_{12}O_{40}]^{3-}$.

Bond-valence sum calculations [36] for **1** indicate that W and Ni are +6 and +2 oxidation states, respectively, and confirm protonated oxygen atoms in the structure. There are only two terminal oxygen ligands, O1W and O2W, which are bonded to Ni3 and Ni6. These terminal ligands are water molecules as indicated by these calculations (the bond valences for O1w and O2w are 0.30 and 0.37, respectively, indicating diprotonation). Six sodium ions as counterions stabilize the polyoxoanion skeleton, so there must be 11 protons in the structure of tungstophosphate anion, which are usually assigned to be delocalized on the whole polyoxoanion for charge balance of the polyoxoanion (results of bond-valence sum calculations are given in Supplementary material).

The structural unit of **2** consists of 10 protons, seven sodium ions, 31 lattice water molecules, and a banana-shaped polyoxoanion $[Co_6P_3W_{24}O_{94}(H_2O)_2]^{17-}$.

3.3. *Magnetic properties*

Temperature-dependent magnetic susceptibility measurements for **2** were performed from 1.8 to 300 K under an external magnetic field of 0.2 T. The temperature dependences of χ_M and $\chi_M T$ are shown in figure 3. The χ_M slowly increases from 0.0626 emu mol^{-1} at 300 K to 0.87 emu mol^{-1} at 18 K, and then rapidly reaches 5.00 emu mol^{-1} at 1.8 K. The $\chi_M T$ product is 18.78 emu K mol^{-1} at 300 K, larger than the spin-only value (11.25 emu K mol^{-1}) expected for six non-interacting high-spin Co^{II} ions ($S = 3/2$) considering $g = 2.0$. The magnetic behavior indicates the presence of the orbital contribution arising from the ground state triplet $^4T_1$ of each Co^{II}, which is known to be significant in an octahedral field [37, 38]. Upon cooling, the $\chi_M T$ product

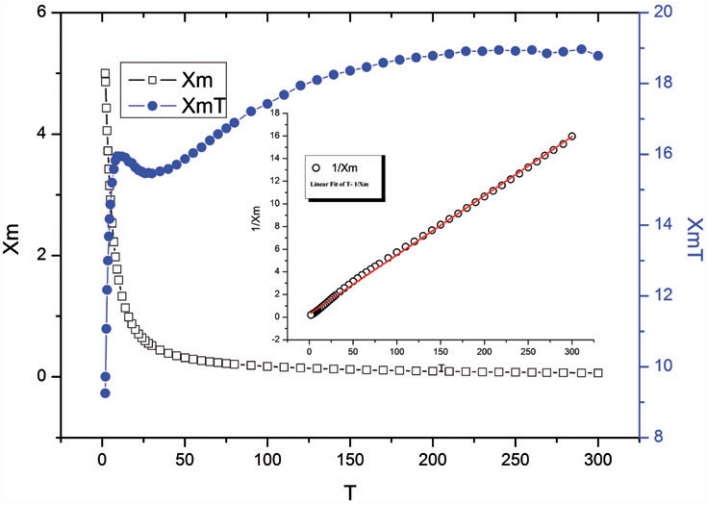

Figure 3. Thermal dependence of the magnetic susceptibility χ_M (bottom) and $\chi_M T$ (top) for **2**. Inserted plots of the temperature dependence of $1/\chi_M$ and the linear fit of the temperature dependence $1/\chi_M$ from 1.8–300 K for **2**, recorded on a powder sample at an applied field of 0.2 T.

gradually decreases to a minimum of 15.76 emu K mol^{-1} at 30 K, and then increases to 15.95 emu K mol^{-1} at 9 K before dropping sharply to 9.25 emu K mol^{-1} at 1.8 K. The decrease at higher temperatures is due to spin-orbit coupling of Co^{II} ions and/or the antiferromagnetic interactions in trinuclear Co^{II} clusters, which is further confirmed by a negative Weiss constant $\theta = -5.24$ K derived from fitting the Curie–Weiss law to the magnetic data between 1.8 and 300 K. The maximum at lower temperatures is indicative of the ferromagnetic Co^{II}–Co^{II} interactions within the trinuclear Co^{II} spin cluster in the sandwich belt [39]. A sudden decrease of the $\chi_M T$ value below 9 K is best ascribed to the large anisotropy of the Co^{II} centers and the presence of zero-field-splitting effects in the ground state [40]. The field dependence of the isothermal magnetization reveals that the magnetization curve at 1.8 K increases with increasing applied field and reaches 7.28 Nμ_B at 9 T without saturation (figure S4). Because of the high anisotropy of the ferromagnetic ground state, this curve does not follow a Brillouin's function behavior [39]. The decrease of the molar magnetic susceptibility at higher temperatures results from spin-orbit coupling of the Co^{II} ion and/or the antiferromagnetic interactions whereas the maximum at the lower temperatures is indicative of the ferromagnetic interactions within the trinuclear Co^{II} spin cluster in the sandwich belt, which is also observed in a cobalt-containing sandwich-type Keggin germanotungstate: $\{[Co(dap)_2(H_2O)]_2[Co(dap)_2]_2[Co_4(Hdap)_2(B\text{-}\alpha HGeW_9O_{34})_2]\} \cdot 7H_2O$ [41].

3.4. *UV spectra*

UV spectrum of **2** shows an absorption at 252 nm assigned to the pπ–dπ charge-transfer transitions of the $O_{b,c} \rightarrow W$ bonds. Compound **2** in aqueous medium (0.2 m mol L^{-1}) at pH = 6.1 is stable for at least 5 days as seen clearly in figure S5.

3.5. *TG spectra*

The TG curves of **1** and **2** (figure S6) show a continual weight loss from 30–800°C. The weight loss at lower temperature (range 30–310°C) is assigned to release of crystal and coordinated water molecules and weight loss from 310 to 700°C corresponds to removal of structural water molecules. The total weight loss of **1** is 10.32% (Calcd 9.98%) and the total weight loss of **2** is 9.78% (Calcd 9.69%).

4. Conclusion

Two new banana-shaped tungstophosphates have been synthesized in aqueous solution and structurally characterized. Magnetic properties of **2** have been measured and analyzed. Currently, we are trying to exploit reactions of the trivacant Keggin $[\alpha\text{-}PW_9O_{34}]^{9-}$ precursors with TM cations.

Supplementary material

CSD 423956 for **1** and CSD 423955 for **2** contain the supplementary crystallographic data for this article. These data can be obtained free of charge from the Fachinformationszentrum Karlsruhe, 76344 Eggenstein-Leopoldsha-fen, Germany; E-mail: crysdata@fizkarlsruhe.de. Supplementary data associated with this article can be found.

Acknowledgments

This work was supported by the Natural Science Foundation of China, Special Research Fund for the Doctoral Program of Higher Education, Innovation Scientists and Technicians Troop Construction Projects of Henan Province, the National Science Fund for Young Scholars of China (Grant no. 21101059) and the Open Research Fund of State Key Laboratory of Inorganic Synthesis and Preparative Chemistry (Grant no. 2011-26).

References

[1] N. Mizuno, M. Misono. *Chem. Rev.*, **98**, 199 (1998).
[2] D.L. Long, E. Burkholder, L. Cronin. *Chem. Soc. Rev.*, **36**, 105 (2007).
[3] C.L. Hill. *Chem. Rev.*, **98**, 1 (1998).
[4] M.I. Khan, E. Yohannes, R.J. Doedens. *Angew. Chem. Int. Ed.*, **38**, 1292 (1999).
[5] J.Y. Niu, D.J. Guo, J.P. Wang, J.W. Zhao. *Cryst. Growth Des.*, **4**, 241 (2004).
[6] J. Chen, T. Lan, Y. Huang, C. Wei, Z. Li, Z. Zhang. *J. Solid State Chem.*, **179**, 1904 (2006).
[7] S. Reinoso, P. Vitoria, J.M.G. Zorrilla, L. Lezama, L.S. Felices, J.I. Beitia. *Inorg. Chem.*, **44**, 9731 (2005).
[8] S. Li, P. Ma, J. Wang, Y. Guo, H. Niu, J. Zhao, J. Niu. *Cryst. Eng. Commun.*, **12**, 1718 (2010).

[9] B. Botar, Y.V. Geletii, P. Kögerler, D.G. Musaev, K. Morokuma, I.A. Weinstock, C.L. Hill. *J. Am. Chem. Soc.*, **128**, 11268 (2006).
[10] C.T. Kressge, M.E. Leonowicz, W.J. Roth, J.C. Vartuni, J.S. Beck. *Nature*, **359**, 710 (1992).
[11] M.A. Aldamen, S.F. Haddad. *J. Coord. Chem.*, **64**, 4244 (2011).
[12] P.T. Ma, Y. Wang, H. Chen, J.P. Wang, J.Y. Niu. *J. Coord. Chem.*, **64**, 2497 (2011).
[13] L.H. Bi, U. Kortz. *Inorg. Chem.*, **43**, 7961 (2004).
[14] R. Khoshnavazi, S. Tayamon. *J. Coord. Chem.*, **63**, 3356 (2010).
[15] S.T. Zheng, D.Q. Yuan, J. Zhang, G.Y. Yang. *Inorg. Chem.*, **46**, 4569 (2007).
[16] Y. Liu, B. Liu, G. Xue, H. Hu, F. Fu, J. Wang. *Dalton Trans.*, 3634 (2007).
[17] J.P. Wang, P.T. Ma, Y. Shen, J.Y. Niu. *Cryst. Growth Des.*, **7**, 603 (2007).
[18] L. Lisnard, P. Mialane, A. Dolbecq, J. Marrot, J.M. Clemente-Juan, E. Coronado, B. Keita, P. deOliveira, L. Nadjo, F. Sécheresse. *Chem. Eur. J.*, **13**, 3525 (2007).
[19] N.H. Nsouli, A.H. Ismail, I.S. Helgadottir, M.H. Dickman, J.M. Clemente-Juan, U. Kortz. *Inorg. Chem.*, **48**, 5884 (2009).
[20] N.H. Nsouli, S.S. Mal, M.H. Dickman, U. Kortz, B. Keita, L. Nadjo, J.M. Clemente-Juan. *Inorg. Chem.*, **46**, 8763 (2007).
[21] J.W. Zhao, Q.X. Han, D.Y. Shi, L.J. Chen, P.T. Ma, J.P. Wang, J.Y. Niu. *J. Solid State Chem.*, **184**, 2756 (2011).
[22] Z. Zhang, Y. Li, E. Wang, C. Qin, H. An. *Inorg. Chem.*, **45**, 4313 (2006).
[23] J.J.B. Almenar, J.M.C. Juan, M.C. Leon, E. Coronado, J.R.G. Mascaros, C.J.G. Garcia. In *Polyoxometalate Chemistry: From Topology Via Self-Assembly to Applications*, M.T. Pope, A. Müller (Eds), p. 234, Kluwer, Dordrecht, The Netherlands (2001).
[24] I.M. Mbomekalle, B. Keita, M. Nierlich, U. Kortz, P. Berthet, L. Nadjo. *Inorg. Chem.*, **42**, 5143 (2003).
[25] M.D. Ritorto, T.M. Anderson, W.A. Neiwert, C.L. Hill. *Inorg. Chem.*, **43**, 44 (2004).
[26] K. Fukaya, T. Yamase. *Bull. Chem. Soc. Jpn.*, **80**, 178 (2007).
[27] J.D. Compain, P. Mialane, A. Dolbecq, I.M. Mbomekallé, J. Marrot, F. Sécheresse, E. Rivière, G. Rogez, W. Wernsdorfer. *Angew. Chem. Int. Ed.*, **48**, 3077 (2009).
[28] B. Li, J.W. Zhao, S.T. Zheng, G.Y. Yang. *Inorg. Chem. Commun.*, **12**, 69 (2009).
[29] R. Tong, L. Chen, Y. Liu, B. Liu, G. Xue, H. Hu, F. Fu, J. Wang. *Inorg. Chem. Commun.*, **13**, 98 (2010).
[30] N. Jiang, F. Li, L. Xu, Y. Li, J. Li. *Inorg. Chem. Commun.*, **13**, 372 (2010).
[31] L. Chen, J. Zhao, P. Ma, Q. Han, J. Wang, J. Niu. *Inorg. Chem. Commun.*, **13**, 50 (2010).
[32] P. Ma, L. Chen, J. Zhao, W. Wang, J. Wang, J. Niu. *Inorg. Chem. Commun.*, **14**, 415 (2011).
[33] SAINT. *Version 6.36 A*, Bruker AXS, Inc., Madison, WI (2002).
[34] G.M. Sheldrick. *SHELXL 97, Version 5.1, Program for Crystal Structure Solution and Refinement*, University of Göttingen, Göttingen, Germany (1997).
[35] M.T. Pope, T.F. Scully. *Inorg. Chem.*, **14**, 953 (1975).
[36] I.D. Brown, D. Altermatt. *Acta Crystallogr. B*, **41**, 244 (1985).
[37] A.V. Palii, B.S. Tsukerblat, E. Coronado, J.M.C. Juan, J.J.B. Almenar. *Inorg. Chem.*, **42**, 2455 (2003).
[38] M.H. Zeng, M.X. Yao, H. Liang, W.X. Zhang, X.M. Chen. *Angew. Chem. Int. Ed.*, **46**, 1832 (2007).
[39] B.S. Bassil, U. Kortz, A.S. Tigan, J.M.C. Juan, B. Keita, P. Oliveira, L. Nadjo. *Inorg. Chem.*, **44**, 9360 (2005).
[40] R.L. Carlin. *Science*, **227**, 129 (1985).
[41] L.J. Chen, D.Y. Shi, J.W. Zhao, Y.L. Wang, P.T. Ma, J.Y. Niu. *Inorg. Chem. Commun.*, **14**, 1052 (2011).